Thermal Degradation Behavior of Styrene-Butadiene-Styrene Tri-Block Copolymer/Multiwalled Carbon Nanotubes Composites

Lan Lu, Haiyang Yu, Shifeng Wang, Yong Zhang

State Key Laboratory of Metal Matrix Composites, School of Chemistry and Chemical Technology, Shanghai Jiao Tong University, 200240 Shanghai, People's Republic of China

ABSTRACT: The thermal degradation behavior of styrene-butadiene-styrene triblock copolymer (SBS) and SBS/multiwalled carbon nanotubes (MWCNTs) composites prepared by solution processing and melt mixing, respectively, was investigated using nonisothermal thermogravimetric analysis (TGA). The kinetic parameters of the activation energy (E_a) for degradation, preexponential factor A, and the reaction order (n) were evaluated by the Flynn-Wall-Ozawa, Kissinger, and Coats-Redfern methods, respectively. E_a increased and n decreased after the incorporation of 3 wt % of MWCNTs into the SBS. The E_a of SBS/MWCNTs composite prepared by melt mixing was higher than that by solution processing, which was attributed to the good dispersion of MWCNTs in SBS and the interactions between MWCNTs and SBS. The gases evolved during thermal degradation at a nitrogen atmosphere were studied by Fourier transform infrared spectroscopy (FTIR) coupled with the TGA. Aliphatic and aromatic C—H peaks appeared simultaneously in FTIR spectra, indicating the thermal degradation of SBS proceeds by a random chain scission process. © 2009 Wiley Periodicals, Inc. J Appl Polym Sci 112: 524–531, 2009

Key words: SBS; multiwalled carbon nanotubes; thermal degradation; kinetics

INTRODUCTION

Carbon nanotubes (CNTs) have been under considerable research since its study first published by Iijima[1] in 1991. They have excellent electrical, thermal, and mechanical properties and are regarded as ultimate nanofillers because of their unique structure. CNTs have been widely incorporated into polymers for various applications,[2,3] for instance, to improve the flammability and thermal stability of polymers.[4,5] The concentration and dispersion of CNTs could significantly affect the thermal properties of polymer/CNTs composites.[6–8] Seo and Park[6] studied the thermal degradation of multiwalled carbon nanotubes (MWCNTs) reinforced polypropylene composites. They found that the activation energies (E_a) of thermal degradation increased with increasing MWCNT content. Besides, CNTs could form a protective layer acting as a heat shield when they were well dispersed in poly(methyl methacrylate). Interfacial bonding between CNTs and polymers could affect the thermal degradation of the composites.[9,10] For instance, the thermal stability of poly-amide 6 filled with amino-functionalized MWCNTs was slightly higher than that with purified MWCNTs.[9] The thermal stability of poly(L-lactide) (PLLA) composite filled with PLLA modified MWCNTs was better than that with pristine MWCNTs.[10] However, the effect of the interfacial bonding between polymers and CNTs on the thermal degradation behavior of CNTs composites has not been extensively studied yet, especially in elastomeric materials.

Styrene-butadiene-styrene triblock copolymer (SBS) has been widely used in various fields because of its outstanding mechanical properties. The applications of SBS include tread, adhesive, asphalt, and plastic modifiers. However, the thermal stability of SBS suffers owing to the sensitivity of the double bonds of polybutadiene (PB) segment in SBS. The chain scission and crosslinking during thermal oxidation are the two main degradation processes of SBS.[11,12] In our previous study, SBS/MWCNTs composites were prepared by two methods, solution processing and melt mixing.[13] It was found that interactions between SBS and MWCNTs occurred during melt mixing, which improved the dispersion of MWCNTs in the SBS matrix as well as the mechanical properties of the SBS composites. In this study, the thermal degradation behavior of SBS and its composites under a nitrogen atmosphere was investigated by nonisothermal thermogravimetric

analysis (TGA). The kinetic parameters were calculated based on TGA curves by the Flynn-Wall-Ozawa,[14] Kissinger,[15] and Coats-Redfern[16] methods, respectively. The effects of the interactions between SBS and MWCNTs and good dispersion of MWCNTs on E_a were discussed. TGA coupled with Fourier transform infrared spectroscopy (FTIR) was also used to investigate the gas evolved during the degradation of SBS/MWCNTs composites.

EXPERIMENTAL

Materials

MWCNTs were produced by Tsinghua Nafine Nano-Power Commercialization Engineering Centre, China and using chemical vapor deposition method. The average diameter of MWCNTs is about 20 nm, and the purity is higher than 95%. SBS (791H, $M_n = 5.9 \times 10^4$, with styrene content at 30%) was supplied by Yueyang General Petrochemical Co., China. Tetrahydrofuran (THF) with reagent purity grade was purchased from Sinopharm Group Chemical Reagent Co. China.

Sample preparation

SBS/MWCNTs composites with 3 wt % of MWCNTs were prepared by two routes: melt mixing at 120°C on a two-roll mill (hereinafter referred as m-SBS/MWCNTs) and via solution processing. For the latter, SBS was dissolved in THF with the ratio of 1 : 9 by weight to form a solution. MWCNTs were separately dispersed in THF under ultrasonication. The SBS solution was poured into the mixture of MWCNTs/THF dispersion. This mixture was under continuously stirred for 4 h. Subsequently, THF was removed by evaporation from the mixture. After the THF was evaporated, the SBS/MWCNTs composite (hereinafter referred as s-SBS/MWCNTs) was obtained as a film.

Characterization

The nonisothermal degradation of SBS and SBS/MWCNTs composites was performed with a TGA 7 analyzer (Perkin–Elmer, Waltham, MA) by heating from 50 to 750°C under a nitrogen atmosphere at a rate of 5, 10, 20, or 40°C/min.

The time-resolved TGA-FTIR analysis was performed from 50 to 750°C at a heating rate of 10°C/min under a nitrogen atmosphere in a TG 209 F1 (Netzsch, Germany) coupled to a Infrared Spectrometer (Tensor 27, Bruker, Germany) equipped with a gas cell, which was heated to 200°C to avoid the condensation of the degradation products inside the transfer line and the gas cell.
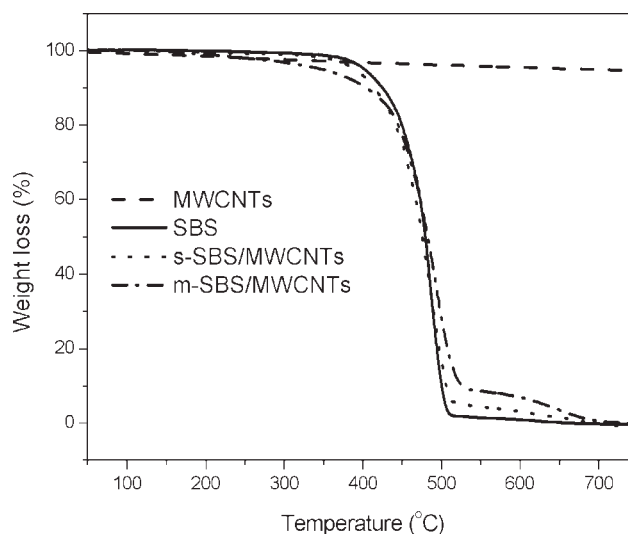

Figure 1 TGA curves of pristine MWCNTs, pure SBS, s-SBS/MWCNTs, and m-SBS/MWCNTs composites at a heating rate of 20°C/min.

RESULTS AND DISCUSSION

In previous study, it was found that the dispersion of nanotubes in m-SBS/MWCNTs was better than that of s-SBS/MWCNTs owing to the high shear force via melt mixing.[13] In addition, the interactions between SBS and MWCNTs occurred during melt mixing, which were supposed to consist of the π–π interaction between MWCNTs and the phenyl groups of SBS as well as the chemical bonding of polybutadiene segments with MWCNTs. This study would focus on the effects of good dispersion and the interactions between MWCNTs and SBS on the thermal properties of the SBS/MWCNTs composites.

TGA curves of pristine MWCNTs, SBS, and their composites at a heating rate of 20°C/min are shown in Figure 1. MWCNTs almost did not suffer degradation up to about 700°C, whereas SBS was completely degraded already at about 500°C. The temperatures corresponding to a weight loss of 5 wt % (T_5) and 50 wt % (T_{50}) of SBS and SBS/MWCNTs composites at different heating rates are shown in Table I. The T_5 and T_{50} values of SBS and s-SBS/MWCNTs for each heating rate are almost similar. However, each T_5 value of m-SBS/MWCNTs is lower than that of pure SBS. This is because chain scission of SBS might occur already during melt mixing so that some SBS with low molecular weight could be formed. In general, T_5 decreases with decreasing the molecular weight of polymers.[17,18] Therefore, the SBS with low molecular weight was easily degraded already at the early stage of the heating process, resulting in the lower T_5 of the m-SBS/MWCNTs. Nevertheless, T_{50} values of m-SBS/MWCNTs at the heating rate of 5, 10, and 20°C/min are higher than that of pure SBS and s-SBS/

TABLE I
T_5 and T_{50} Values of SBS and SBS/MWCNTs Composites

Heating rate (°C/min)	SBS		s-SBS/MWCNTs		m-SBS/MWCNTs	
	T_5 (°C)	T_{50} (°C)	T_5 (°C)	T_{50} (°C)	T_5 (°C)	T_{50} (°C)
5	376	456	375	456	319	460
10	385	466	383	462	322	471
20	402	479	391	475	342	483
40	412	489	413	494	344	493

MWCNTs. The residual weight of m-SBS/MWCNTs at 600°C, when the heating rate is 20°C/min, is about 7%, which is higher than that of SBS (1%) and s-SBS/MWCNTs (3%). This is probably due to the interactions between SBS and MWCNTs, so that MWCNTs may favor to form thermal shield to decrease external heat flux and then protect SBS from degradation at higher temperature, leading to the improvement of thermal stability of SBS composites.[7,19]

Nonisothermal measurements at different heating rates (5, 10, 20, and 40°C/min) are performed to study the relationship between kinetic parameters and conversion.[20] The TGA and differential thermogravimetric (DTG) curves for SBS and its composites are shown in Figures 2 and 3, respectively. DTG curves indicate that a weight-loss stage occurred during degradation. It is interesting that a small peak appears around 590°C in the DTG curve of m-SBS/MWCNTs at the heating rate of 5°C/min, which cannot be observed either in SBS or s-SBS/MWCNTs. This is because SBS and MWCNTs may form a char, which could protect the underlying layer. This char was relatively stable when temperature was low and it was degraded at high temperature.

TGA data was analyzed using a single step kinetics equation:

$$\beta\frac{d\alpha}{dT} = Af(\alpha)\exp\left(-\frac{E_a}{RT}\right) \quad (1)$$

where, β is the heating rate, α the conversion which is the inverse of weight loss, T the temperature, A the preexponential factor, and R the universal gas
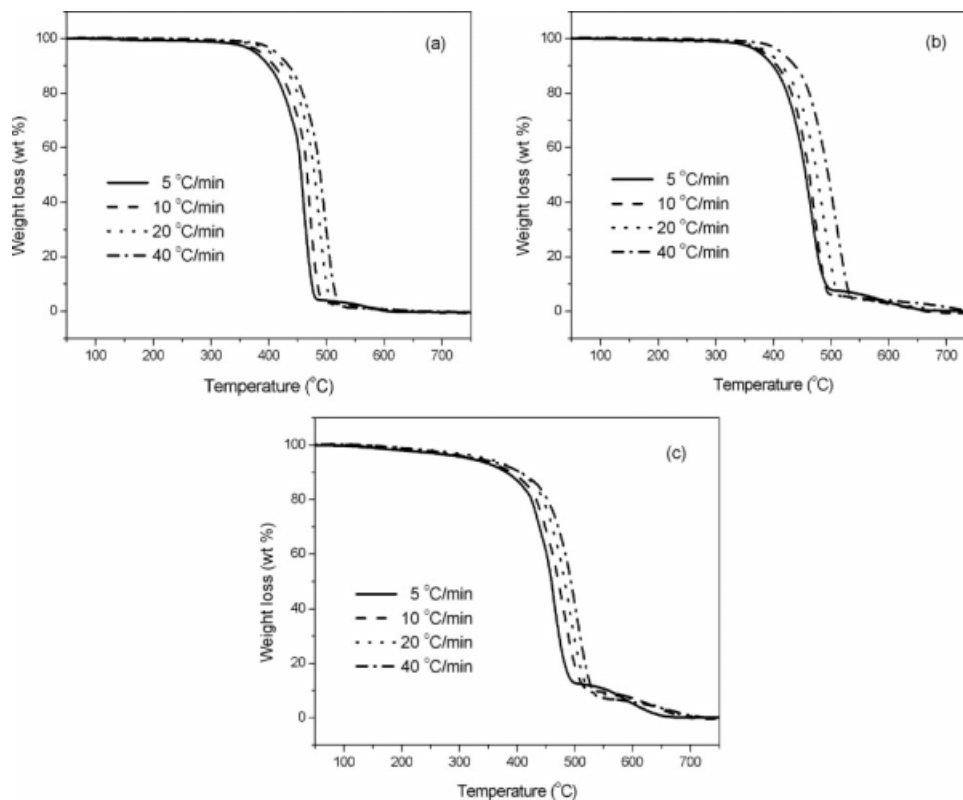

Figure 2 TGA curves of pure SBS (a), s-SBS/MWCNTs (b), and m-SBS/MWCNTs composites (c) at heating rates of 5, 10, 20, and 40°C/min.
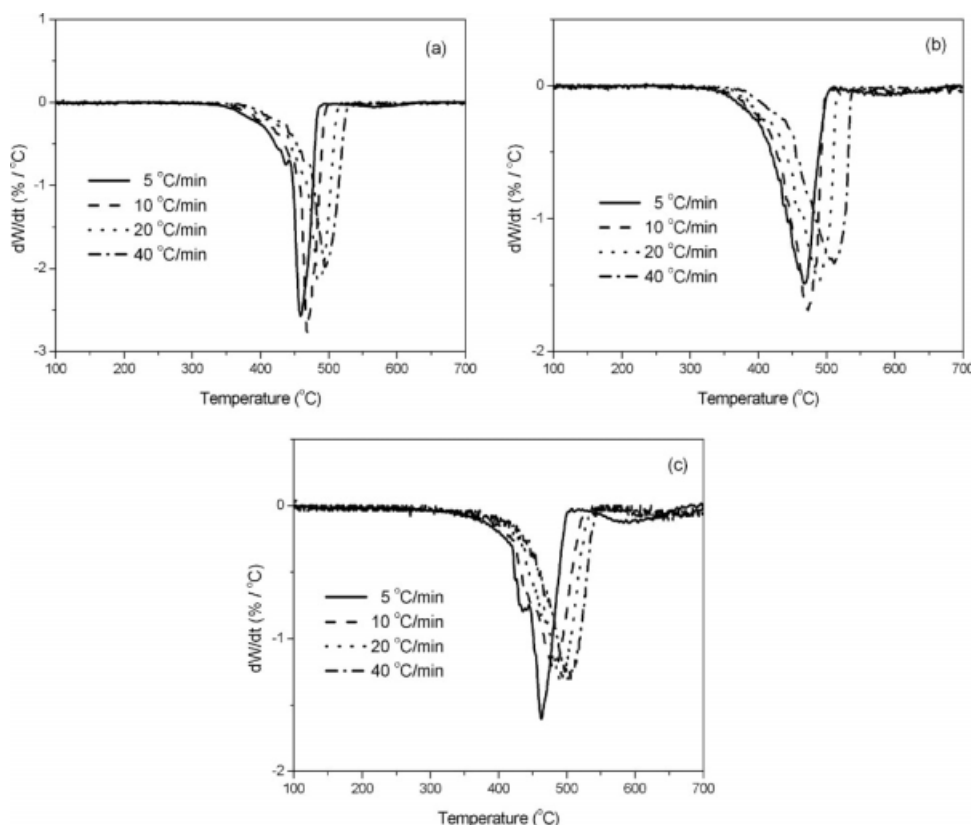
Figure 3 DTG curves of SBS (a), s-SBS/MWCNTs (b), and m-SBS/MWCNTs composites (c) at different heating rates of 5, 10, 20, and 40°C/min.

constant ($8.314 \text{ J mol}^{-1}\text{K}^{-1}$). $f(\alpha)$ is a function of α depending on the mechanism of the degradation reaction, which can be expressed by following equation:

$$f(\alpha) = (1 - \alpha)^n \quad (2)$$

where n is the reaction order.

E_a is determined by using the Flynn-Wall-Ozawa method. Equation (1) was integrated to eq. (3).

$$\ln \beta - \ln \frac{AE_a}{RF(\alpha)} - 5.331 - 1.052 \frac{E_a}{RT} \quad (3)$$

where,

$$F(\alpha) = \int_0^\alpha \frac{d\alpha}{(1-\alpha)^n} \quad (4)$$

is the integral conversion function. For given α, a plot of $\ln \beta$ versus $(1/T)$ should be a straight line whose slope allows the evaluation of E_a. The plots determined by the Flynn-Wall-Ozawa method for SBS and SBS/MWCNTs composites are shown in Figure 4. The fitted lines at different α are approximately parallel to each other and all the correlation coefficients are around -0.99. The mean values of E_a of the SBS, the s-SBS/MWCNTs, and the m-SBS/

MWCNTs composites calculated from these plots are 227, 228, and 269 kJ/mol, respectively. There is a little difference between E_a of the pure SBS and the s-SBS/MWCNTs, indicating that the low loading of MWCNTs into SBS hardly influences the E_a of SBS. However, the E_a of m-SBS/MWCNTs is much higher than that of SBS or s-SBS/MWCNTs.

E_a can also be determined by using the Kissinger method described by eq. (5):

$$\ln \frac{\beta}{T_{max}^2} = \ln \frac{nAR(1 - \alpha_{max})^{n-1}}{E_a} - \frac{E_\alpha}{RT_{max}} \quad (5)$$

where, T_{max} is the temperature corresponding to the inflection point at the maximum degradation rate determined from the DTG curves. It is assumed that α_{max} at T_{max} is constant. E_a can be calculated from the slope of $\ln \beta/T_{max}^2$ as a function of $1/T_{max}$ (Fig. 5). The E_a of SBS and its composites are 238, 254, and 294 kJ/mol, respectively. The m-SBS/MWCNTs composite with 3 wt % MWCNTs has the highest value of E_a, which is in agreement with the trend as obtained from the Flynn-Wall-Ozawa method.

The n of the nonisothermal degradation process can be determined also by the Kissinger method[21]:
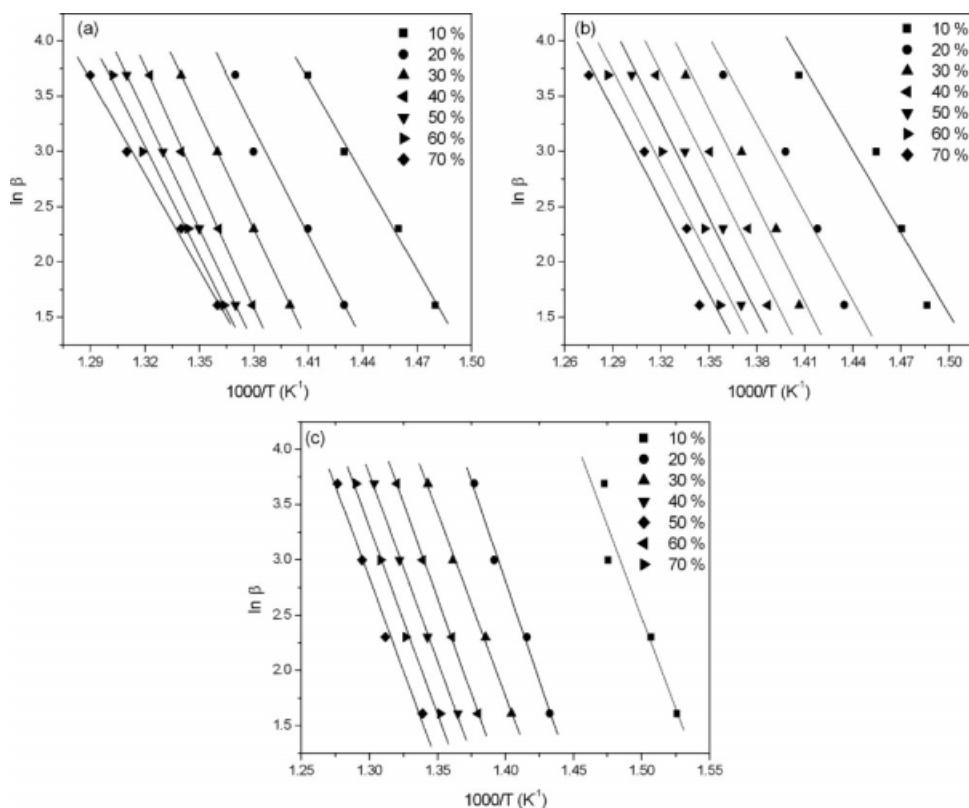
$$n = 1.26\sqrt{S} \quad (6)$$

Figure 4 Plots for the determination of the activation energy E_a at different conversion for the pure SBS (a), s-SBS/MWCNTs (b), and m-SBS/MWCNTs composites (c) according to the Flynn-Wall-Ozawa method.

where, S is the shape index of the DTG curves, which can be obtained by eq. (7):

$$S = \frac{a}{b} \qquad (7)$$

where, a and b are calculated from the DTG curves at the inflection point, as shown in Figure 6.

The values of n at different heating rates for SBS and its composites are listed in Table II. The n varies with the heating rates for SBS and is ~ 1 for SBS/MWCNTs composites. E_a and ln A can be obtained by the Coats-Redfern method using the eq. (8).
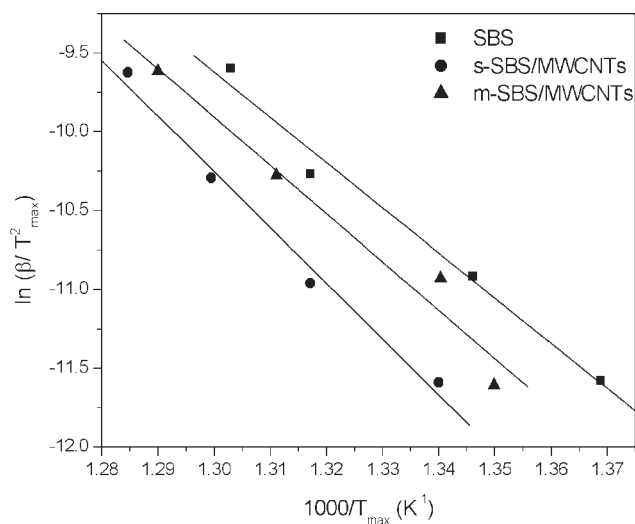

Figure 5 Plots for the determination of the activation energies E_a at different conversion for pure SBS, s-SBS/MWCNTs, and m-SBS/MWCNTs composites according to the Kissinger method.
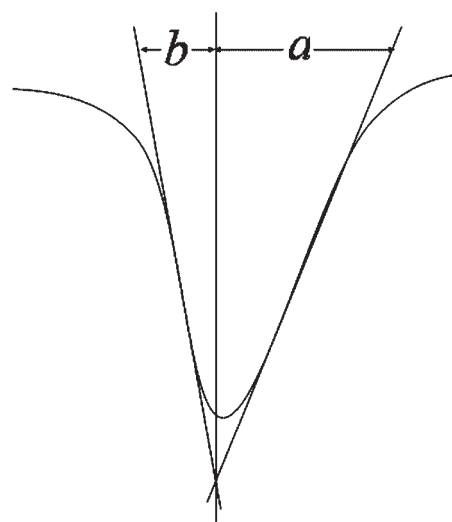

Figure 6 Schematic diagram for the calculation of the parameters and in shape index as obtained from DTG curves. a and b are the absolute values of the slopes of tangents to the curve at the inflection points.

TABLE II
Summary of the Reaction Order *n*, Activation Energy E_a, and Logarithm of the Preexponential Factor ln *A* Calculated From Kissinger and Coats-Redfern Methods for SBS and its Composites

	Heating rate (°C/min)	n	E_a (kJ/mol)	ln A
SBS	5	2.0	119	10.4
	10	1.8	121	11.0
	20	1.4	122	11.5
	40	1.3	118	11.0
s-SBS/MWCNTs	5	1.0	144	14.8
	10	0.9	127	12.2
	20	0.9	124	11.9
	40	0.9	120	11.3
m-SBS/MWCNTs	5	1.4	159	17.4
	10	1.1	135	13.0
	20	1.0	138	14.1
	40	1.0	156	17.4

$$\ln \frac{F(\alpha)}{T^2} = \ln\left[\frac{AR}{\beta E_\alpha}\left(1 - \frac{2RT}{E_\alpha}\right)\right] - \frac{E_\alpha}{RT} \cong \ln \frac{AR}{\beta E_\alpha} - \frac{E_\alpha}{RT} \tag{8}$$

The different expressions of $F(\alpha)$ corresponding to n are given in Table III. The $\ln F(\alpha)/T^2$ for various values of α are plotted as a function of $1/T$ to give a straight line whose slope and intercept are E_a and ln A, respectively.

E_a and ln A vary with n, as seen in Table II. The mean values of E_a of SBS, s-SBS/MWCNTs, and m-SBS/MWCNTs are 120, 129, and 147 kJ/mol, respectively. The E_a calculated from three methods are summarized in Table IV. The values of E_a vary with the kinetics model used. E_a for SBS, s-SBS/MWCNTs, and m-SBS/MWCNTs obtained from the Coats-Redfern method are lower than the corresponding ones from the Flynn-Wall-Ozawa and the Kissinger methods. But they all show the same trends, i.e., E_a increases when adding MWCNTs. E_a of m-SBS/MWCNTs is always the highest among the three samples independent of the selected methods. Flynn-Wall-Ozawa and the Kissinger methods are model-free methods by using several different heating rates regardless the degradation model, whereas Coats-Redfern method is model-fitting method by using a given single heating rate. Kinetics parameters depend on the selected methods.[22] Based

on a set of TGA curves recorded at different heating rates, it is reported that the model-free methods are considered to provide consistent information on the degradation mechanism involved and should lead to reliable kinetic parameters.[23] In addition, because of the almost similar values obtained by Flynn-Wall-Ozawa and Kissinger methods, it is believed that E_a data calculated by these methods reflect the actual kinetic parameters more than the data calculated by the Coats-Redfern method.

When adding a filler into a polymer, the interactions between the polymer and the filler may lead to several chemical and physical processes, including bound rubber and rubber shell formation, occlusion and filler networking.[24] One or some of these processes can take place depending on the nature of the filler and polymer, which ultimately could influence the degradation processing of the polymer matrix.[25–27] It is reported that the E_a of polypropylene filled with acetylated sisal fiber is higher than that of composites filled with untreated ones: a possible explanation of this behavior might be the higher polymer-filler interaction, which results in improved stability of the composites.[25] The interactions between the filler and the polymer could help to develop a hard and compact char layer, which increases the resistance under flame stress.[26,27] Some researches also show that polymer/CNT composites with stronger interactions between the polymer and the CNTs have higher E_a compared with composites having weaker interactions between polymer and CNTs.[9,10] For instance, the thermal stability of polyamide 6 filled with amino-functionalized MWCNTs was slightly higher than that with purified MWCNTs.[9] The E_a of PLLA composite filled with PLLA-g-MWCNT was obviously higher than that with pristine MWCNTs.[10] The authors believed that the interactions between polymer and modified MWCNTs played an important role for the further improvement of the thermal stability of the composites. In our previous study, it is found that the interactions between SBS and MWCNTs, during melt mixing, and that the dispersion of MWCNTs in m-SBS/MWCNTs was better than that of s-SBS/MWCNTs. It is inferred that the interactions

TABLE III
Integral Expressions for the Different Reaction Orders *n*

n	$f(\alpha)$	$F(\alpha)$
1	$1-\alpha$	$-\ln(1-\alpha)$
1.5	$(1-\alpha)^{3/2}$	$2[(1-\alpha)^{-1/2}-1]$
2	$(1-\alpha)^2$	$(1-\alpha)^{-1}-1$

TABLE IV
Summary of the Activation Energies E_a Calculated by Different Methods

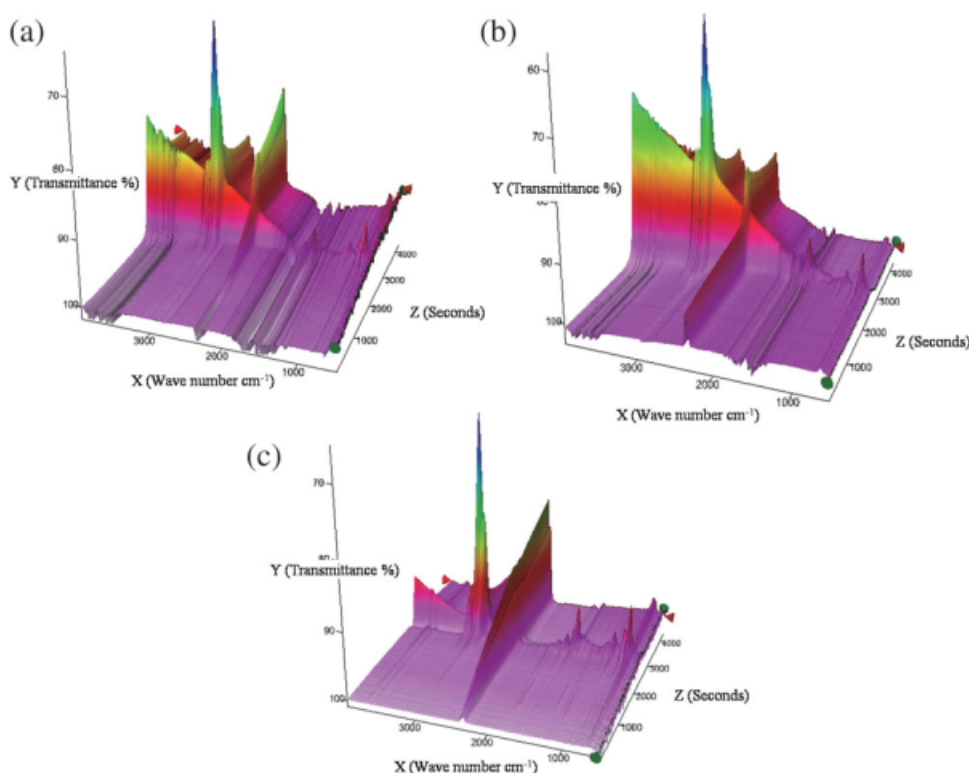| Model	Flynn-Wall-Ozawa (mean value)	Kissinger	Coats-Redfern (mean value)
	E_a (kJ/mol)		
SBS	227	238	120
s-SBS/MWCNTs	228	254	129
m-SBS/MWCNTs	269	294	147

Figure 7 Time-resolved FTIR spectra of the degradation products of SBS (a), s-SBS/MWCNTs (b), and m-SBS/MWCNTs composites (c). [Color figure can be viewed in the online issue, which is available at www.interscience.wiley.com].

between SBS and MWCNTs and the good dispersion of MWCNTs are responsible for the significantly higher E_a of the m-SBS/MWCNTs composite compared with s-SBS/MWCNTs.

Time-resolved FTIR spectra obtained during the degradation process of SBS and its composites under a nitrogen atmosphere are shown in Figure 7. Figure 8 shows the *in situ* FTIR spectra of degradation products at each weight loss. The absorption peaks of hydrocarbons appear when α is about 5%. The peak at 1453 cm^{-1} corresponds to the C—H deformation vibration and 908 cm^{-1} to the out-of-plane bending. The peaks at 2932–2870 cm^{-1} and 3072–3033 cm^{-1} are characteristic of aliphatic and aromatic C—H stretching. They show quantitative changes during the degradation process. Aliphatic and aromatic C—H peaks show up simultaneously when α is about 5%, indicating the thermal degradation of SBS proceeds by a random chain scission process.[28] When α reaches 90%, the aromatic C—H peaks of SBS and s-SBS/MWCNTs almost disappear but aliphatic ones still remain, which is ascribed to the higher thermal stability of PB than that of PS at high temperatures.[29] However, the aromatic C—H stretching peak of m-SBS/MWCNTs can still be observed when α is 90%, indicating that the thermal degradation rate of the m-SBS/MWCNTs composite is lower than that of the pure SBS and s-SBS/MWCNTs composite. This is probably because the

interactions between SBS and MWCNTs and good dispersion of MWCNTs in the case of m-SBS/MWCNTs could hinder molecular motion, and the diffusion speed of degradation products became slow, therefore, the aromatic C—H stretching peak can still be observed in high conversion.[30,31]

CONCLUSIONS

The initial degradation temperature at 5 wt % weight loss of the SBS/MWCNTs composite prepared by melt mixing was lower than that of SBS and SBS/MWCNTs composites prepared by solution processing. The analysis of the thermal degradation kinetic parameters of SBS and its composites calculated by the Flynn-Wall-Ozawa, Kissinger, and Coats-Redfern methods, receptively, showed that the activation energy increased after the addition of MWCNTs. The SBS/MWCNTs composite prepared by melt mixing had the higher activation energy than SBS and SBS/MWCNTs composite prepared by solution processing independent of three calculation methods. The reaction order decreased after the addition of MWCNTs in the SBS matrix. Experiments performed in a nitrogen atmosphere by TGA coupled with FTIR indicated that the thermal degradation of SBS proceeds by a random chain scission process.
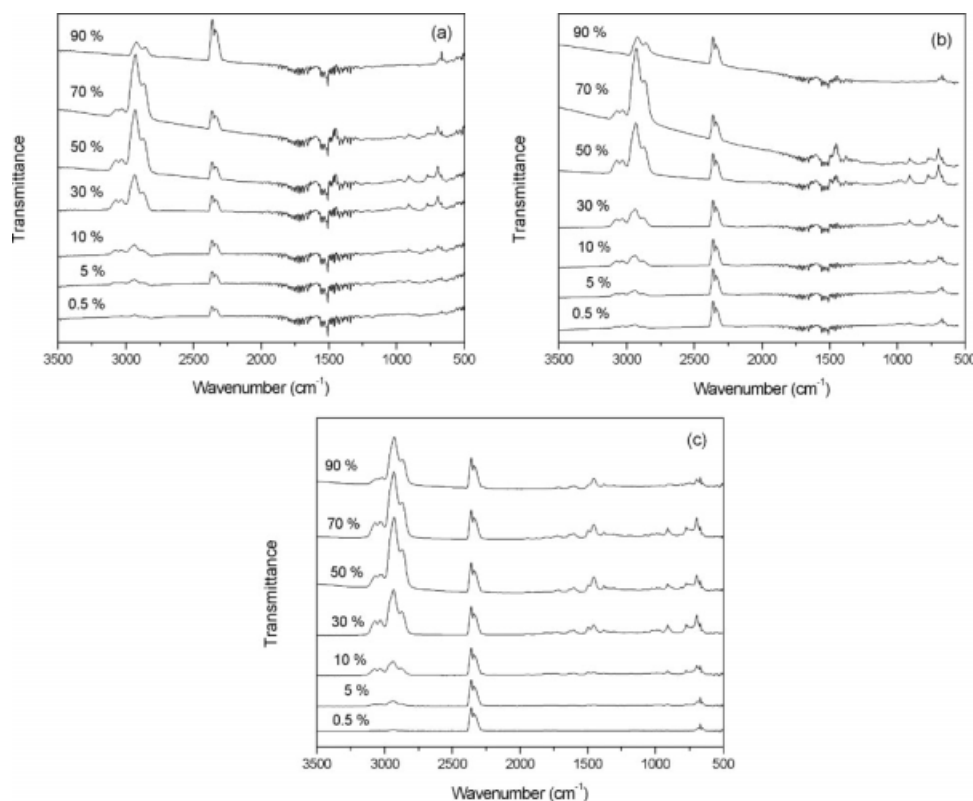
Figure 8 TGA-FTIR spectra at different conversions for SBS (a), s-SBS/MWCNTs (b), and m-SBS/MWCNTs composites (c).

References

1. Iijima, S. Nature 1991, 354, 56.
2. Baughman, R. H.; Zakhidov, A. A.; De Heer, W. A. Science 2002, 297, 787.
3. Dai, H. Surf Sci 2002, 500, 218.
4. Breuer, O.; Sundararaj, U. Polym Compos 2004, 25, 630.
5. Coleman, J. N.; Khan, U.; Gun'ko, Y. K. Adv Mater 2006, 18, 689.
6. Seo, M. K.; Park, S. J. Macromol Mater Eng 2004, 289, 368.
7. Kashiwagi, T.; Du, F.; Winey, K. I.; Groth, K. M.; Shields, J. R.; Bellayer, S. P.; Kim, H.; Douglas, J. F. Polymer 2005, 46, 471.
8. Bourbigot, S.; Duquesne, S.; Jama, C. Macromol Symp 2006, 233, 180.
9. Li, J.; Tong, L.; Fang, Z.; Gu, A.; Xu, Z. Polym Degrad Stab 2006, 91, 2046.
10. Kim, H. S.; Hyun Park, B.; Yoon, J. S.; Jin, H. J. Eur Polym J 2007, 43, 1729.
11. Munteanu, S. B.; Brebu, M.; Vasile, C. Polym Degrad Stab 2005, 89, 501.
12. Xu, J.; Zhang, A.; Zhou, T.; Cao, X.; Xie, Z. Polym Degrad Stab 2007, 92, 1682.
13. Lu, L.; Zhou, Z.; Zhang, Y.; Wang, S.; Zhang, Y. Carbon 2007, 45, 2621.
14. Tkaeo, O. Bull Chem Soc Jpn 1965, 38, 1881.
15. Kissinger, H. E. J Res Natl Bur Stand 1956, 57, 217.
16. Coast, A.; Redfern, J. Nature 1964, 201, 68.
17. Lin, J. J.; Shau, S. M.; Wei, K. M. Polym Degrad Stab 2000, 70, 171.
18. Wang, X. S.; Li, X. G.; Yan, D. Polym Degrad Stab 2000, 69, 361.
19. Kashiwagi, T.; Grulke, E.; Hilding, J.; Harris, R.; Awad, W.; Douglas, J. Macromol Rapid Commun 2002, 23, 761.
20. Doyle, C. D. J Appl Polym Sci 1961, 5, 285.
21. Kissinger, H. E. Anal Chem 1957, 29, 1702.
22. Pisharath, S.; Ang, H. G. Thermochim Acta 2007, 458, 26.
23. Budrugeac, P. Polym Degrad Stab 2000, 71, 185.
24. Mohanraj, G. T.; Vikram, T.; Shanmugharaj, A. M.; Khastgir, D.; Chaki, T. K. J Mater Sci 2006, 41, 4777.
25. Albano, C.; Gonzalez, J.; Ichazo, M.; Kaiser, D. Polym Degrad Stab 1999, 66, 179.
26. Liufu, S. C.; Xiao, H. N.; Li, Y. P. Polym Degrad Stab 2005, 87, 103.
27. Kim, S. J Polym Sci Part B: Polym Phys 2003, 41, 936.
28. Hacaloglu, J.; Ersen, T.; Ertugrul, N.; Fares, M. M.; Suzer, S. Eur Polym J 1997, 33, 199.
29. Suzuki, M.; Wilkie, C. A. Polym Degrad Stab 1995, 47, 217.
30. Yang, S.; Castilleja, J. R.; Barrera, E. V.; Lozano, K. Polym Degrad Stab 2004, 83, 383.
31. Chen, E. C.; Wu, T. M. Polym Degrad Stab 2007, 92, 1009.